

## Preclinical report

# Characteristics of etoposide-induced apoptotic cell death in the U-937 human lymphoma cell line

Petra Martinsson,<sup>1</sup> Gunnar Liminga,<sup>1</sup> Peter Nygren<sup>2</sup> and Rolf Larsson<sup>1</sup>

<sup>1</sup>Department of Medical Sciences, Division of Clinical Pharmacology, and <sup>2</sup>Department of Oncology, Radiology and Clinical Immunology, University Hospital, Uppsala University, 751 85 Uppsala, Sweden.

Cell death induced by etoposide in the human lymphoma cell line U-937 GTB was characterized. Activity of caspases -3, -8 and -9 was measured by spectrophotometric detection of specific cleavage products, DNA fragmentation by TdT-mediated dUTP nick end-labelling (TUNEL), and apoptotic morphology by conventional staining and microscopy, as well as by a novel method—the microculture kinetics (MiCK) assay. Synthesis of protein and DNA during exposure was monitored by incorporation of radioactive leucine and thymidine, respectively. The effects of caspase inhibitors on total viability, as well as early and late morphological changes were studied. Etoposide rapidly induced apoptosis, dependent on caspase-3 and -8, but inhibition of these caspases did not prevent major cell death, but promoted a switch in late morphology. The novel MiCK assay added valuable information on early morphological events during cell death. Hence, this study provides support for caspase-8-mediated apoptosis in U-937 GTB when exposed to etoposide. General caspase inhibition switches cell death to one with a different morphology. [© 2001 Lippincott Williams & Wilkins.]

**Key words:** Anticancer treatment, apoptosis, caspases, CHS 828, etoposide, human lymphoma.

## Introduction

Overwhelming evidence that anti-tumoral drugs kill malignant cells by inducing apoptotic cell death has accumulated over the past 10 years.<sup>1–6</sup> Apoptosis is a genetically conserved cell death program, ultimately leading to stereotypic morphological features, such as membrane blebbing, nuclear condensation and fragmentation.<sup>7</sup> This physiological mode of cell death,

crucial during normal development and tissue homeostasis, allows the organism to eliminate damaged, infected or dying cells without an inflammatory response. Aberrant cell death signaling can cause, for example, malignancy and autoimmune disease. The apoptotic program is generally believed to be initiated either via cell surface receptors [CD95/Fas or tumor necrosis factor (TNF)-RI] or damage to DNA, or other vital cellular structures, and is propagated by key proteases, known as caspases.<sup>8–10</sup> Caspase-8<sup>11</sup> and -9<sup>12</sup> are the most apical caspases of separate, yet not entirely exclusive pathways.<sup>13</sup> Eventually they both activate caspase-3, -6 and/or -7,<sup>14</sup> leading to DNA degradation, one of the hallmarks of apoptosis,<sup>15,16</sup> and to the typical morphology of apoptosis. Other events in the programmed cell death course may or may not be dependent on caspase activity.<sup>13,17–19</sup>

Etoposide is a semisynthetic podophyllotoxin derivative, described to inhibit topoisomerase II.<sup>20</sup> Its mechanism of action starts with stabilization of covalent topoisomerase II-DNA complexes and induction of DNA double-strand breaks in the vicinity of these complexes, subsequently leading to activation of stress-associated signaling pathways, cell cycle arrest and activation of caspases.<sup>21</sup> Previous reports have described various parts of the apoptotic cell death pathway induced by etoposide in the human lymphoma cell line U-937.<sup>15,22–26</sup>

The present study was undertaken to further characterize etoposide-induced apoptotic cell death in U-937 GTB cells. The kinetics of protein and DNA synthesis, as well as the involvement of the separate signaling pathways, represented by caspase-8 and -9, respectively, were addressed. Conventional morphology, kinetic monitoring of cell cultures and total viability measurements were used as endpoints for caspase dependency.

Correspondence to P Martinsson, Division of Clinical Pharmacology, University Hospital, 751 85 Uppsala, Sweden.  
Tel: (+46) 18 611 1010; Fax: (+46) 18 51 92 37;  
E-mail: petra.martinsson@medsci.uu.se

## Materials and methods

### Cells

The histiocytic lymphoma cell line U-937 GTB,<sup>27</sup> harvested during logarithmic growth, was used for all experiments. The cells were maintained in RPMI 1640 medium (without phenol red for microculture kinetic (MiCK) experiments; Sigma-Aldrich, Irvine, UK), supplemented with 10% heat-inactivated fetal bovine serum (Sigma-Aldrich), 2 mM glutamin, 50 µg/ml streptomycin and 60 µg/ml penicillin (Sigma-Aldrich). Cell culture flasks were kept in a controlled humidified atmosphere of 37°C, 5% CO<sub>2</sub>. Cultures were monitored and passaged twice weekly. Etoposide was obtained from the hospital pharmacy (as Vepesid; Bristol-Myers Squibb, Bromma, Sweden) and was used at 25 µM for all experiments.

### TdT-mediated dUTP nick end-labelling (TUNEL)

Cytospin slides of U-937 GTB cells, continuously exposed to 25 µM etoposide [or phosphate buffered saline (PBS) for control slides] in a culture flask at a cell density of  $5 \times 10^5$  cells/ml, were prepared and kept in -20°C and thawed prior to analysis. TUNEL was performed stringent to the commercial protocol (*In situ* cell death detection kit, fluorescein; Boehringer Mannheim, Mannheim, Germany). In brief, cytospin preparations were fixed in 4% formaldehyde for 30 min, rinsed with PBS, and permeabilized in a solution of 0.1% Triton X-100 and 0.1% sodium citrate for 2 min. After rinsing twice with PBS the labeling reaction was allowed to take place under Parafilm M for 60 min under standard incubation conditions (37°C, controlled humidified atmosphere with 5% CO<sub>2</sub>, protected from light). The slides were rinsed in PBS, air-dried and mounted with antifade mounting medium (Vectashield; Vector, Burlingame, CA) and coverslips. Analysis of TUNEL staining was performed in a confocal microscope and the experiment was repeated 3 times. TUNEL-positive and -negative cells from two random visual fields from each experiment were counted.

### Detection of DNA and protein synthesis

Synthesis of DNA and protein was measured by detecting the incorporation of radio labeled thymidine or leucine, respectively. A Cytostar-T plate (*In Situ* mRNA Cytostar-T assay' kit; Amersham International, Little Chalfont, UK), which is a pre-made scintillating microtiter plate with scint fluid molded into the

bottom of the wells,<sup>28,29</sup> was used. Cells were collected by centrifugation and suspended in fresh culture medium containing 111 nCi/ml [<sup>14</sup>C]thymidine (Amersham CFA.532, 56 mCi/mmol, 50 µCi/ml) for DNA synthesis experiments or 222 nCi/ml [<sup>14</sup>C]leucine (Amersham CFB.183, 56 mCi/mmol, 50 µCi/ml) for protein synthesis experiments, yielding a final radioactivity in the wells of approximately 20 and 40 nCi, respectively. Aliquots of 180 µl cell suspension containing  $5 \times 10^4$  cells were added to each well. Blank wells received only medium containing isotope. Etoposide, synthesis inhibitors or PBS (blank and untreated control wells) were added in duplicates (20 µl/well) 2 h after cell seeding when the measured radioactivity in cell containing wells was at least twice the baseline value. Positive synthesis inhibition controls received 10 µg/ml aphidicholine (DNA synthesis experiments) or 5 µg/ml cycloheximide (protein synthesis experiments). Radioactivity was measured using a Wallac 1450 MicroBeta triluX liquid scintillation counter (Wallac, Turku, Finland) with MicroBeta Windows workstation software (Wallac).

### Detection of the activity of caspase-3, -8 and -9

Caspase activity was assayed by colorimetric detection of *p*-nitroanilidine (pNA) after cleavage of the peptide substrates DEVD-pNA, IETD-pNA or LEHD-pNA for caspases-3, -8 and -9, respectively. The reagents were part of a 'Caspase-8 Colorimetric Assay' or 'Caspase-9 Colorimetric Assay' (R&D Systems, Minneapolis, MN), except DEVD-pNA (from ApoAlert caspase-3 colorimetric assay kit; Clontech, Palo Alto, CA).

Cells were exposed to etoposide for up to 4 h in culture flasks at a cell density of  $2.5 \times 10^5$  cells/ml (cells from a flask not exposed served as control). Aliquots of  $2 \times 10^6$  cells were collected in duplicates by centrifugation 1, 2 and 4 h after start of exposure. Supernatants were removed by aspiration and pellets were frozen and kept in -70°C, for a maximum of 4 weeks until analysis. The pellets were thawed and lysis induced by 10 min exposure to 100 µl cell lysis buffer, on ice. After 3 min of centrifugation at 12 000 g, 50 µl of the protein containing cell lysate was transferred to a microtiter plate with flat-bottomed wells. Subsequently, 50 µl of reaction buffer with 1% dithiothreitol was added, together with 5 µl of the pNA substrates (yielding final concentrations of 48 nM of DEVD-pNA or 190 µM of IETD-pNA and LEHD-pNA). Blank wells received 100 µl reaction buffer and 5 µl substrate. Absorbance was measured at 405 nm in an ELISA reader (SpectraMax Plus; Molecular Devices, Sunny-

vale, CA) after 90 min incubation at 37°C, protected from light. Activity was calculated as (mean of test duplicates – mean of blanks)/(mean controls – mean of blanks) and expressed as percentages.

#### Investigation of caspase dependency

Ninety-six-well microtiter plates were prepared with 10  $\mu$ l 500  $\mu$ M etoposide for test triplicates (final exposure concentration 25  $\mu$ M), and 20  $\mu$ l PBS for blanks and controls (six of each), and kept at –70°C. At the start of an experiment one flat-bottomed microtiter plate and one with V-shaped well bottoms were thawed and 10  $\mu$ l of either caspase inhibitor was added in triplicates at 20 times the desired final concentration (12.5–50  $\mu$ M). DEVD-fmk (sequence Asp-Glu-Val-Asp-CH<sub>2</sub>F; Clontech) is a cell-permeable, irreversible inhibitor of caspase-3 and Z-Asp-CH<sub>2</sub>-DCB (Z-Asp-CH<sub>2</sub>[(2,6-dichlorobenzoyl)oxy]methane; Calbiochem, La Jolla, CA) is a cell-permeable, irreversible general caspase inhibitor. Aliquots of 180  $\mu$ l U-937 GTB cells (111 000/ml) were seeded into the V-shaped microtiter plate which was placed in a regular incubator at 37°C, 5% CO<sub>2</sub> in humidified air. Cytospin slides for morphologic examination were prepared from designated wells at selected time points and stained with May-Grünwald/Giemsa. After 72 h the fluorometric microculture cytotoxicity assay (FMCA) was performed. This total viability assay has been described in detail previously<sup>30</sup> and is based on measurement of fluorescence generated by the intracellular hydrolysis of fluorescein diacetate (FDA) to fluorescein by cells with preserved membrane integrity, after 72 h of continuous drug exposure at standard incubation conditions. The results are presented as survival indices (SI), defined as the fluorescence in experimental wells as percent of that in control wells, with blank values subtracted.

#### MICK assay

Characterizing cell death through detecting changes in cell morphology by monitoring absorbance of undisturbed cell cultures was recently developed and validated.<sup>31,32</sup> Control cultures of proliferating cells show a steady increase in absorbance, whereas cultures undergoing necrosis exhibit a lowering in absorbance followed by a plateau. Apoptotic cultures display a steep increase, exceeding that of controls, and a subsequent decrease and plateau phase, each representing cellular and nuclear condensation, initial post-apoptotic cellular disintegration and cell debris. A flat-bottomed microtiter plate was seeded with 180  $\mu$ l aliquots of 555 000 cells/ml and placed in a regular

incubator for 30 min for gas and temperature equilibration, and subsequently each well was layered with 50  $\mu$ l sterile mineral oil (Sigma, St Louis, MO). Absorbance at 600 nm was measured automatically every 14 min for 48 h in a SpectraMAX Plus 96-well microtiter plate spectrophotometer (Molecular Devices) at 37°C.

#### Data presentation and statistics

The unpaired *t*-test was employed for all calculations of statistical significance. Calculations were performed on raw data with blank values subtracted.

## Results

The TUNEL protocol was performed on U-937 GTB cells continuously exposed to 25  $\mu$ M etoposide for up to 8 h to investigate whether this *in situ* method can detect the DNA fragmentation previously shown by agarose gel electrophoresis in this system. The cells formed large aggregates, and showed extensive chromatin condensation, nuclear fragmentation and increasing TUNEL positivity (Figure 1). The extent of these changes was time dependent (Table 1).

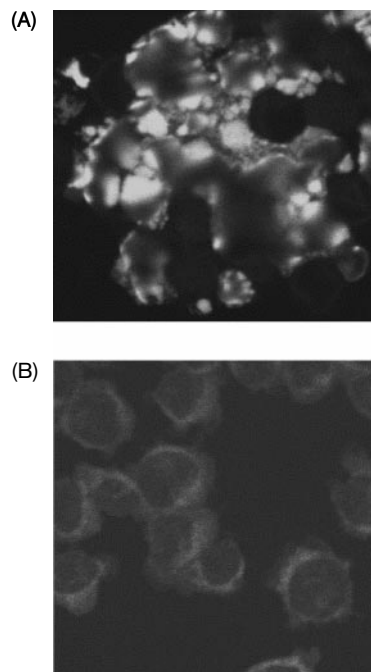


**Figure 1.** TUNEL staining in U-937 GTB cells exposed to 25  $\mu$ M etoposide for 4 h (A) or untreated control cells at the same time point (B). Shown as 50% of  $\times 40$  magnification.

U-937 GTB cells exposed to etoposide promptly ceased to synthesize DNA, although the suppression of DNA synthesis was not as complete as for cells exposed to the specific DNA synthesis inhibitor aphidicholin (Figure 2A). Protein synthesis, on the other hand, was largely unaffected by etoposide for 4 h, then tapered off (Figure 2B) and reached a plateau at 20 h (not shown).

**Table 1.** Percentage of TUNEL-positive cells after continuous exposure to 25  $\mu$ M etoposide

Exposure time (h)	TUNEL-positive cells [% (SD)]
2.5	6 (9)
4	49 (6)
8	100 (0)

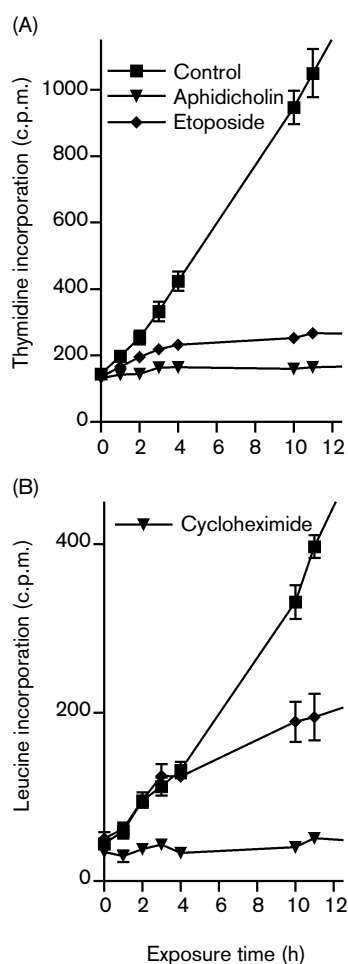


**Figure 2.** Whole cell synthesis of DNA (A) and protein (B) assessed in U-937 GTB cells assessed by incorporation of radioactive thymidine and leucine, respectively. Data points represent the mean of three or four consecutive experiments ( $\pm$  SEM).

Colorimetric detection of caspase activity, rather than the presence of the cleaved proteases, was used to investigate the patterns of involved caspases. Continuous exposure of U-937 GTB cells to etoposide for up to 2 h produced no increase in activity of the investigated caspases (Figure 3). After 4 h the activity of caspase-3 was greatly increased compared to control ( $p < 0.001$ ) as was, albeit to a lesser degree, caspase-8 activity ( $p < 0.001$ ). For caspase-9 no statistically significant activation was observed during this period (Figure 3).

The morphology of U-937 GTB cells continuously exposed to etoposide for 5 h was characterized by chromatin condensation, nuclear fragmentation, cell shrinkage and grouping of affected cells (Figure 4A). Blocking caspase activity in etoposide-exposed cells resulted in dramatically altered morphology. Co-incubation with the specific caspase-3 cleavage inhibitor DEVD-fmk for 5 h at 12.5  $\mu$ M resulted in increased membrane blebbing, inhibited cell shrinkage and an altered pattern of nuclear fragmentation in a majority of the cells (Figure 4B). At 25  $\mu$ M the same pattern in a smaller proportion of the cells was apparent (Figure 4C), and 50  $\mu$ M resulted in complete inhibition of nuclear fragmentation and cellular aggregation, while remaining membrane blebbing (Figure 4D). Similar results were evident when cells were co-incubated with the pancaspase inhibitor Z-Asp-CH<sub>2</sub>-DCB (not shown). DEVD-fmk did not significantly affect total viability compared to etoposide

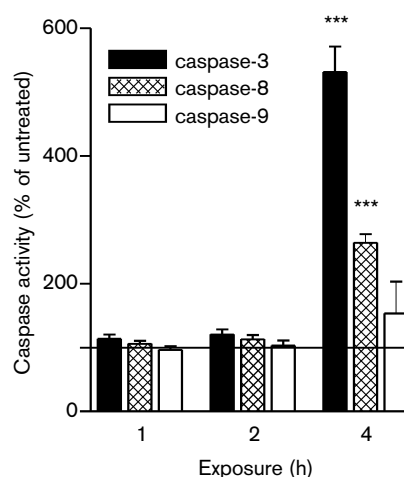


**Figure 3.** The activity of caspases in U-937 GTB cells exposed to 25  $\mu$ M etoposide for the indicated time periods. Results are expressed as percentages of the activity in untreated control cells (indicated by horizontal line). Activity was measured as optical density of the respective caspases' colored cleavage products. Means of three consecutive experiments, with error bars representing SEM. \*\*\* $p < 0.001$ .

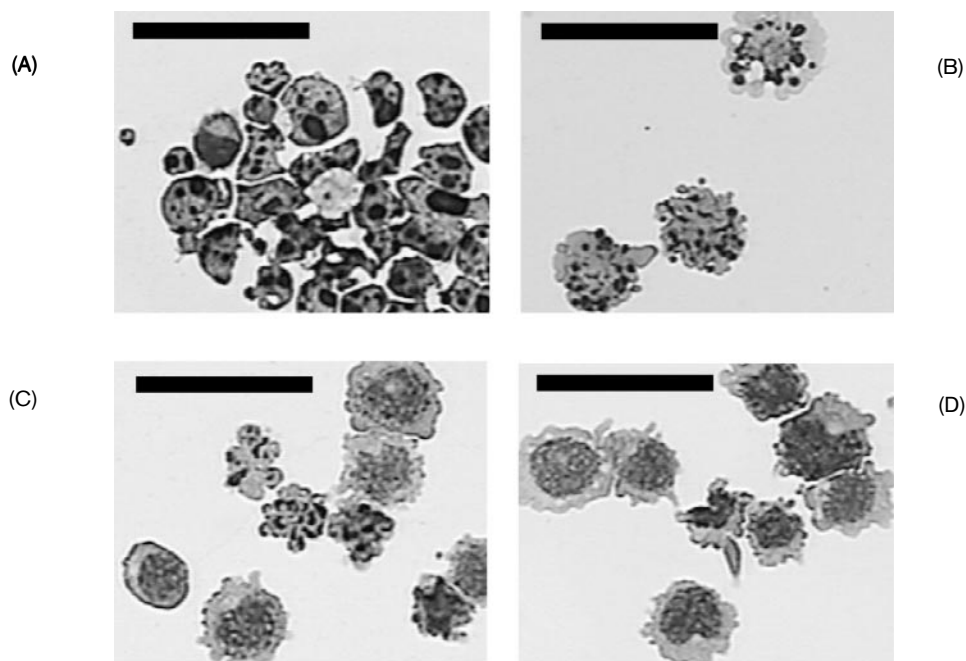


**Figure 4.** U-937 GTB cells stained with May–Grünwald/Giemsa and photographed at  $\times 40$  magnification in a Nikon ECLIPSE E400 microscope fitted with a Sony Exwave HAD digital color video camera. Cells were exposed for 4 h to 25  $\mu\text{M}$  etoposide only (A) or co-incubated with the caspase inhibitor DEVD-fmk at 12.5 (B), 25 (C) or 50 (D)  $\mu\text{M}$ . Size bars=50  $\mu\text{m}$ .

exposure alone, as measured by the FMCA, while 50 M Z-Asp-CH<sub>2</sub>-DCB slightly increased cell viability ( $p < 0.005$ ). However, total viability remained low (Table 2). To further characterize the effect of the inhibitors, kinetics of crude morphology of U-937 GTB cells continuously exposed to etoposide was monitored by the MiCK assay (Figure 5). For etoposide alone there was an early peak in absorbance, followed promptly by a lowered plateau as the cells die and disintegrate, a typical MiCK pattern of apoptotic cell cultures. Adding increasing concentrations of DEVD-fmk caused a prolongation of the process, with a less steep increase of absorbance and wider peaks. However, there were still obvious MiCK signs of apoptotic processes at inhibitor concentrations resulting in complete prevention of apoptotic features as judged by morphology.

## Discussion

It has been established that when U-937 cells are exposed to etoposide, caspases are cleaved and thereby activated.<sup>13,15,22,23</sup> Further downstream, endonucleases<sup>15,25,26</sup> are activated and together they are ultimately responsible for the observed morphological features of apoptosis and the cells eventually die. However, inhibition of endonucleases does not pre-

**Table 2.** Survival index (SI) for cells exposed to etoposide alone or in combination with indicated caspase inhibitors (inh)

	SI [% (SD)]	
	DEVD	Z-Asp
Etoposide 25 $\mu\text{M}$	1.0 ( $\pm 0.4$ )	0.4 ( $\pm 0.2$ )
Etoposide + inh 12.5 $\mu\text{M}$	3.7 ( $\pm 1.6$ )	1.0 ( $\pm 0.7$ )
Etoposide + inh 25 $\mu\text{M}$	5.7 ( $\pm 3.9$ )	2.4 ( $\pm 1.5$ )
Etoposide + inh 50 $\mu\text{M}$	6.9 ( $\pm 4.2$ )	6.8 ( $\pm 1.7$ ) <sup>a</sup>

<sup>a</sup> $p < 0.005$ .

vent cell death,<sup>26</sup> suggesting that apoptotic nuclear morphology and cell death are partially independent of one another *in vitro*.

Caspase-3 has been shown to be the key actor<sup>13,23</sup> and accelerates etoposide-induced apoptosis.<sup>33</sup> In addition caspases -7, -8 and -9 are cleaved as shown by immuno blotting.<sup>13,34</sup> The semi-quantitative method for detecting caspase activity in the present study confirms a massive activation of caspase-3. It is generally believed that cytotoxic drugs, including etoposide, induced activation of caspase-3 following from activation of caspase-9 and the 'mitochondrial' pathway of apoptosis.<sup>13,34</sup> The present results contradicts this notion and indicate that the cleavage of caspase-9 is not necessary for etoposide activity, and

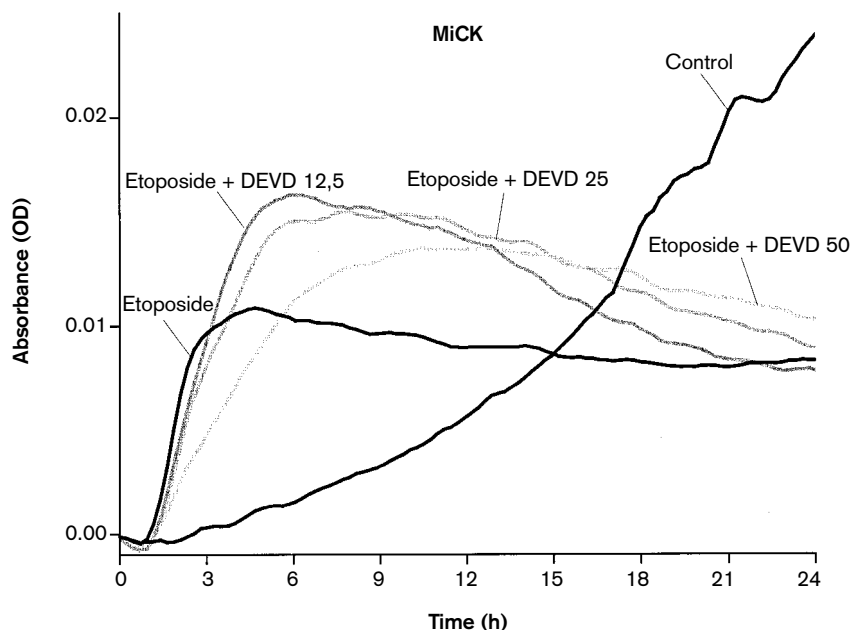


**Figure 5.** One representative MiCK assay out of four separate experiments, showing the effect in U-937 GTB cells exposed to etoposide alone and combined with the indicated concentrations of the caspase inhibitor DEVD-fmk.

leads us to conclude that caspase-9 may not be the main activator of caspase-3 in etoposide-induced apoptosis in U-937 GTB cells.

The theory that in some cell lines, etoposide treatment leads to upregulation of CD95/CD95 ligand and the activation of the apoptosis pathway starting with caspase-8<sup>35</sup> has received well founded criticism (reviewed in Kaufmann<sup>21</sup>). However, we show that protein synthesis is unaffected during the first 4 h of exposure, which would allow for such an upregulation. More convincingly, Wesselborg<sup>36</sup> recently demonstrated that caspase-8 is activated in cells exposed to etoposide, irrespective of CD95 status. The caspase activity pattern observed in the present study suggests a similar route of action in U-937 GTB cells. In the present study we also demonstrate that simple TUNEL staining confirms the etoposide-induced DNA fragmentation previously shown with DNA gel electrophoresis.<sup>36</sup>

A variety of protease inhibitors have been shown to circumvent the different features of the apoptotic process induced by etoposide in U-937 cells. Mashima was the first to show that apoptosis was blocked by Z-Asp<sup>22</sup> and Fujita later showed that this effect was due to suppressed caspase-3 activation.<sup>33</sup> DEVD was shown to prevent DNA fragmentation.<sup>23</sup> We demonstrated that these two inhibitors suppress apoptotic morphology in a dose-dependent manner, assessed by conventional morphology. However, although the

apoptotic features were not visible to the eye, there was obvious remaining cellular and/or nuclear condensation detectable by the novel MiCK assay. According to this method it seems clear that the cells are still significantly affected by etoposide, at inhibitor concentrations approaching toxic levels. This clearly adds to the information obtained by regular morphologic examination. In addition, neither inhibitor substantially prevented cell death, indicating either that the commitment to cell death lies upstream of these events or that a less apparent form of apoptosis is allowed to proceed.

## Conclusion

In summary, the present investigation of the effects of etoposide on U-937 GTB morphology and cell death suggests that caspase inhibitors partly prevent nuclear apoptotic features, but does not inhibit cell death *per se*. It also indicates that the etoposide-induced apoptotic response involves the caspase-8-associated apoptosis pathway.

## References

1. Hickman J. Apoptosis induced by anticancer drugs. *Cancer Metast Rev* 1992; 2: 121-39.

2. Hannun Y. Apoptosis and the dilemma of cancer chemotherapy. *Blood* 1997; **89**: 1845-53.
3. Huschtscha L, Bartier W, Malmström A, Tattersall M. Cell death by apoptosis following anticancer drug treatment *in vitro*. *Int J Oncol* 1995; **6**: 585-93.
4. Kerr J, Winterford C, Harmon B. Apoptosis. Its significance in cancer and cancer therapy. *Cancer* 1994; **73**: 2013-26.
5. Lutzker SG, Levine AJ. Apoptosis and cancer chemotherapy. *Cancer Treat Res* 1996; **87**: 345-56.
6. Kaufmann S, Earnshaw W. Induction of apoptosis by cancer chemotherapy. *Exp Cell Res* 2000; **256**: 42-9.
7. Kerr JF, Wyllie AH, Currie AR. Apoptosis: a basic biological phenomenon with wide-ranging implications in tissue kinetics. *Br J Cancer* 1972; **26**: 239-57.
8. Earnshaw W, Martins L, Kaufmann S. Mammalian caspases: structure, activation, substrates, and functions during apoptosis. *Annu Rev Biochem* 1999; **68**: 383-424.
9. Nunez G, Benedict MA, Hu Y, Inohara N. Caspases: the proteases of the apoptotic pathway. *Oncogene* 1998; **17**: 3237-45.
10. Harvey NL, Kumar S. The role of caspases in apoptosis. In: Sheper T, ed. *Advances in biochemical engineering and biotechnology*. Berlin: Springer 1998: 107-28.
11. Salvesen GS. Caspase 8: igniting the death machine. *Structure Fold Des* 1999; **7**: R225-9.
12. Kuida K. Caspase-9. *Int J Biochem Cell Biol* 2000; **32**: 121-4.
13. Sun XM, MacFarlane M, Zhuang J, Wolf BB, Green DR, Cohen GM. Distinct caspase cascades are initiated in receptor-mediated and chemical-induced apoptosis. *J Biol Chem* 1999; **274**: 5053-60.
14. Porter AG, Jänicke RU. Emerging roles of caspase-3 in apoptosis. *Cell Death Different* 1999; **6**: 99-104.
15. Ghibelli L, Maresca V, Coppola S, Gualandi G. Protease inhibitors block apoptosis at intermediate stages: a compared analysis of DNA fragmentation and apoptotic nuclear morphology. *FEBS Lett* 1995; **377**: 9-14.
16. Darzynkiewicz Z, Traganos F. Measurement of apoptosis. *Adv Biochem Eng Biotechnol* 1998; **62**: 33-73.
17. Han Z, Bhalla K, Pantazis P, Hendrickson EA, Wyche JH. Cif (cytochrome *c* efflux-inducing factor) activity is regulated by Bcl-2 and caspases and correlates with the activation of Bid. *Mol Cell Biol* 1999; **19**: 1381-9.
18. Bossy-Wetzel E, Newmeyer DD, Green DR. Mitochondrial cytochrome *c* release in apoptosis occurs upstream of DEVD-specific caspase activation and independently of mitochondrial transmembrane depolarization. *EMBO J* 1998; **17**: 37-49.
19. Kagan VE, Fabisiak JP, Shvedova AA, *et al*. Oxidative signaling pathway for externalization of plasma membrane phosphatidylserine during apoptosis. *FEBS Lett* 2000; **477**: 1-7.
20. Hande KR. Etoposide: four decades of development of a topoisomerase II inhibitor. *Eur J Cancer* 1998; **34**: 1514-21.
21. Kaufmann SH. Cell death induced by topoisomerase-targeted drugs: more questions than answers. *Biochim Biophys Acta* 1998; **1400**: 195-211.
22. Mashima T, Naito M, Fujita N, Noguchi K, Tsuruo T. Identification of actin as a substrate of ICE and an ICE-like protease and involvement of an ICE-like protease but not ICE in VP-16-induced U937 apoptosis. *Biochem Biophys Res Commun* 1995; **217**: 1185-92.
23. Dubrez L, Savoy I, Hamman A, Solary E. Pivotal role of a DEVD-sensitive step in etoposide-induced and Fas-mediated apoptotic pathways. *EMBO J* 1996; **15**: 5504-12.
24. Dini L, Coppola S, Ruzittu M, Ghibelli L. Multiple pathways for apoptotic nuclear fragmentation. *Exp Cell Res* 1996; **223**: 340-7.
25. Garcia-Bermejo L, Perez C, Vilaboa NE, de Blas E, Aller P. cAmp increasing agents attenuate the generation of apoptosis by etoposide in promonocytic leukemia cells. *J Cell Sci* 1998; **111**: 637-44.
26. Shrivastava P, Sodhi A, Ranjan P. Anticancer drug-induced apoptosis in human monocytic leukemic cell line U937 requires activation of endonuclease(s). *Anti-Cancer Drugs* 2000; **11**: 39-48.
27. Sundström C, Nilsson K. Establishment and characterization of a human histiocytic lymphoma cell line (U-937). *Int J Cancer* 1976; **17**: 565-77.
28. Harris DW, Kenrick MK, Pither RJ, Anson JG, Jones DA. Development of a high-volume *in situ* mRNA hybridization assay for the qualification of gene expression utilizing scintillating microplates. *Anal Biochem* 1996; **243**: 249-56.
29. Graves R, Davies R, Brophy G, O'Beirne G, Cook N. Noninvasive, real-time method for the examination of thymidine uptake events—application of the method to V-79 cell synchrony studies. *Anal Biochem* 1997; **248**: 251-7.
30. Larsson R, Kristensen J, Sandberg C, Nygren P. Laboratory determination of chemotherapeutic drug resistance in tumor cells from patients with leukemia, using a fluorometric microculture cytotoxicity assay (FMCA). *Int J Cancer* 1992; **50**: 177-85.
31. Kravtsov VD, Greer JP, Whitlock JA, Koury MJ. Use of microculture kinetic assay of apoptosis to determine chemosensitivities of leukemias. *Blood* 1998; **92**: 968-80.
32. Kravtsov V, Daniel T, Koury M. Comparative analysis of different methodological approaches to the *in vitro* study of drug-induced apoptosis. *Am J Pathol* 1999; **155**: 1327-39.
33. Fujita N, Tsuruo T. Involvement of Bcl-2 cleavage in the acceleration of VP-16-induced U937 cell apoptosis. *Biochem Biophys Res Commun* 1998; **246**: 484-8.
34. Garrido C, Bruey JM, Fromentin A, Hammann A, Arrigo AP, Solary E. HSP27 inhibits cytochrome *c*-dependent activation of procaspase-9. *FASEB J* 1999; **13**: 2061-70.
35. Friesen C, Fulda S, Debatin KM. Cytotoxic drugs and the CD95 pathway. *Leukemia* 1999; **13**: 1854-8.
36. Wesselborg S, Engels IH, Rossmann E, Los M, Schulze-Osthoff K. Anticancer drugs induce caspase-8/FLICE activation and apoptosis in the absence of CD95 receptor/ligand interaction. *Blood* 1999; **93**: 3053-63.

(Received 15 May 2001; accepted 12 June 2001)